Journal of Zhejiang University SCIENCE A
ISSN 1009-3095 (Print); ISSN 1862-1775 (Online)
www.zju.edu.cn/jzus; www.springerlink.com
E-mail: jzus@zju.edu.cn

Effect of processing parameters on the electromagnetic radiation emission during plastic deformation and crack propagation in copper-zinc alloys*

KUMAR Rajeev‡, MISRA Ashok

(*Department of Mechanical Engineering, Birla Institute of Technology, Mesra, 835215, Ranchi, India*)

E-mail: rajivk1091@rediffmail.com; dr_ashok_misra@rediffmail.com

Received Mar. 20, 2006; revision accepted Aug. 8, 2006

Abstract: This paper presents some investigations on the effect of processing parameters on the emission of electromagnetic radiation (EMR) during plastic deformation and crack propagation in copper-zinc alloys. Timing of the EMR emissions, maximum stress during crack instability, stress-intensity factor, elastic strain energy release rate, maximum EMR amplitude, RMS value of EMR amplitude, EMR frequency and electromagnetic energy release rate were analysed for the effect of rolling directions at different percentage of zinc content in Cu-Zn alloy specimens. The same parameters were also analysed for 68-32 Cu-Zn alloy specimens at different annealing temperatures and at different angles θ, to the rolling direction. EMR emissions are observed to be highly anisotropic in nature. At θ=45° to 60°, marked changes in mechanical and electromagnetic parameters were observed. Specimens annealed at 500 °C, just above the recrystallization temperature, and at 700 °C, when grain-size growth is rapid, EMR responses have been found to have well-defined patterns.

Key words: Radiation, Plastic deformation, Rolling direction, Annealing, Fracture
doi:10.1631/jzus.2006.A1800 **Document code:** A **CLC number:** TG139.7

INTRODUCTION

The physics of plastic deformation and crack propagation at atomic level is complex but is essential for the development of new materials. This requires an understanding of the atomic level phenomena associated with the plastic deformation. In this context, emission of electromagnetic radiation (EMR) during plastic deformation and crack propagation in metals and alloys, and generation of transient magnetic fields during crack initiation in ferromagnetic materials are reported in (Misra, 1973; 1975a; 1975b; 1976; 1977; 1978; 1981; Misra and Ghosh, 1980a; 1980b; Misra and Varshney, 1990; Misra and Kumar, 2004; Mishra and Misra, 1980). Srilakshmi and Misra (2005a) also reported additional phenomenon of secondary EMR emission during plastic deformation and crack propagation in uncoated and metal-coated metallic materials. These results have helped in designing and developing smart sensors (Srilakshmi and Misra, 2005d; Kumar and Misra, 2006).

Plastic deformation features are known to be greatly influenced by the processing history of the metallic materials. Therefore, investigations were carried out to study the effect of processing parameters on the EMR emissions in Cu-Zn alloys which have a wide range of applications. Effects of two basic processing parameters have been studied: (1) effect of zinc addition on EMR emission along different rolling directions, and (2) effect of annealing temperature on EMR emissions along different rolling directions, and the results are presented in this paper.

EMR EMISSION

In order to make the presentation comprehensive,

‡ Corresponding author
* Project supported by Department of Science and Technology, India

the phenomenon of EMR emission is described briefly. Misra (1975a; 1975b; 1976; 1977; 1978) reported that EMR is emitted from metals and alloys during pronounced transient changes in the dislocation structure, which occur, for example near the yield point, start of work hardening, crack initiation and propagation, and fracture. EMR has recordable amplitude varying from a few mV to 1 V depending upon the antenna design, and has a wide range of frequency spectrum.

Molotskii (1980) considered these stages of pronounced transient changes in the dislocation structure where a multiplication of dislocations can occur, where various reactions can occur between dislocations, and where there is a significant change in the dislocation density. Since long-range electric fields exist near dislocations in metals, the appearance of accelerated dislocations could result in the emission of EMR. Based on the dynamics of edge dislocations in a viscous medium, he calculated a limiting EMR frequency in the MHz region as reported by Misra (1978).

Jagasivamani (1987), and Jagasivamani and Iyer (1988) confirmed and explored this new effect further and reported maximum energy bursts in kHz range in heat-treated spring steel. Tudik and Valuev (1980) reported EMR emission of rather large frequency during fracture of iron and aluminium. Using photomultiplier, they were able to detect EMR at wavelengths from ~300 to >1500 nm for iron and its alloys and from ~650 to >1500 nm for aluminum and its alloys.

Misra and Ghosh (1980) showed, both theoretically and experimentally, that the RMS value of EMR amplitude bears a parabolic relation with the Debye frequency of metals. Further, EMR peak voltage varies linearly with bond energy of metals while frequency varies parabolically with the bond energy; EMR amplitude and frequency decrease with increase in lattice parameter (Misra and Kumar, 2004).

The experimental research shows that the EMR signals (voltage vs time graph) emitted from the metallic materials investigated, are of two broad nature: (1) exponentially decaying, and (2) damped sinusoidal. This conclusion is important in the sense that they reflect upon the dynamics of dislocation-solute, and dislocation-electron interactions during plastic deformation and crack propagation in metallic materials.

EXPERIMENTAL PROGRAM

Materials and specimens

Hard rolled 68-32 brass sheets were used for the investigations on the effect of rolling directions on EMR emissions. For the effect of zinc addition, ingots of Cu-Zn alloys with 10%, 20%, 30%, and 40% zinc content, were cold rolled by 90% reduction, in the sheet forms. These alloy sheets were fabricated in the National Metallurgical Laboratory, Jamshedpur, India. Test specimens of dimensions 100 mm×14 mm×1 mm were prepared with their longitudinal axis at angles θ=0°, 30°, 45°, 60°, and 90°, to the rolling direction of sheets.

For the effect of annealing temperature tests, specimens of dimensions 100 mm×14 mm×1 mm were cut with their longitudinal axis along the rolling direction of hard rolled 68-32 brass sheet. Sets of specimens were annealed for 2 h at 200 °C, 500 °C, and 700 °C respectively.

An initial single edge straight notch of length a=7 mm (corresponding to an initial notch length, a, to specimen width, w, ratio a/w=0.5 as per fracture test standards) was provided at the centre of each specimen with the help of a jeweller's scissor to ensure Mode I fracture when loaded under tension.

Instrumentation

A horizontal portable 2 ton capacity Hounsfield tensometer was employed for loading. Two copper chips of dimensions 10 mm×10 mm×0.2 mm, pasted on insulation paper, were fixed onto the specimen. These chips were joined electrically and thus acted as an antenna. The electrical cable of the antenna was connected to a 150 MHz analog-digital HAMEG oscilloscope model HM1507-3 with built-in software SP107FFT (Beta-version) for recording the signals. This software had fast Fourier Transform (FFT) facility to convert the time domain EMR signals into frequency domain. An IBM Pentium IV personal computer was used for data storage and processing. An RS 232 interface was used for transferring the data from the oscilloscope to the computer. Further details of the instrumentation can be obtained from (Srilakshmi and Misra, 2005a; 2005b; 2005c).

Parameters for evaluation

All specimens were fractured under Mode I

(opening or tensile mode, where the crack surfaces move directly apart). Therefore, a total of seven parameters were measured and evaluated for the study: maximum stress at the crack tip instability S_{uc}, stress-intensity factor K_I, elastic strain energy release rate G_I, maximum EMR amplitude $|V_{pmax}|$, RMS voltage of each EMR signal V_{RMS}, minimum dominant frequency f, and electromagnetic energy release rate A.

RESULTS AND DISCUSSIONS

Parameters

The stress-intensity factor K_I for the specimen configuration shown in Fig.1, is given by (Hertzberg, 1996),

$$K_I=[(P\sqrt{a})/(wh)][1.99-0.41(a/w)+18.7(a/w)^2 -38.48(a/w)^3+53.85(a/w)^4], \quad (1)$$

where P is the maximum load and h, the thickness of the sheet.

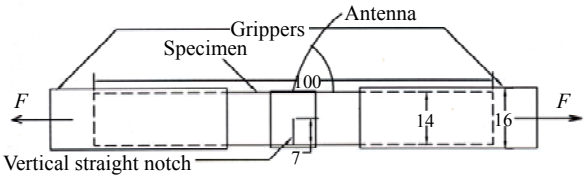

Fig.1 Specimen configuration with antenna position (All dimensions in mm)

The elastic strain energy release rate G_I for plane-stress condition is given by (Hertzberg, 1996),

$$G_I=K_I^2/E, \quad (2)$$

where E is the Young's modulus of elasticity of the specimen material. Since E is the function of both composition and texture, the values of E which ranged from 95 GPa to 103 GPa, were experimentally determined for each composition and texture, and used in the evaluation of G_I.

The energy or power in the time-domain representation is equal to the energy or power in the frequency-domain. Energy is used for nonperiodic time-domain signals, while power applies to periodic time-domain signals. The energy spectrum of a signal is defined as the square of the magnitude spectrum (Haykin and van Veen, 2002). Hence for the evaluation of average energy release rate A, the EMR signal V_p vs time graph was converted into V_p^2 vs time plot through the in-built software in the oscilloscope. The maximum V_p signal was selected for the evaluation of A. If the time duration of this maximum V_p signal is Δt, the average EMR energy release rate A can be calculated from the following equation:

$$A=\frac{\int V_p^2 \mathrm{d}t}{\Delta t} =\frac{\text{area below the } V_{pmax}^2-\text{time, curve portion}}{\Delta t}. \quad (3)$$

It may be noted here that EMR is emitted during the movement of accelerated dislocations through the material. Therefore, each EMR signal corresponds to different energized state of the dislocation hence the maximum EMR amplitude $|V_{pmax}|$, should correspond to the highest energized state. On the other hand, if EMR emission is supposed to be the cumulative effect of the dislocations then V_{RMS} should be an important factor but evaluation of energy release rate becomes difficult. It is for this reason, V_{pmax} portion of the EMR signal was selected for the evaluation of A (for example, portion $ABCDE$ in Fig.2).

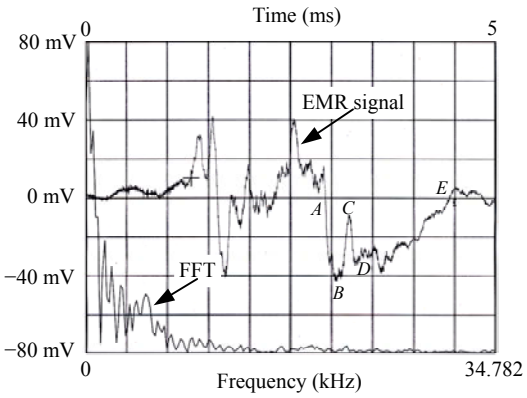

Fig.2 EMR signal with its FFT superimposed, emitted during Mode I fracture of 1.0 mm thick 68-32 brass sheet

Experimental observations revealed that the emitted EMR signals contain mixed frequency components. Therefore, minimum dominant EMR fre-

quency was selected for the study of the effect of processing parameters on EMR emissions for consistency of analysis.

In general, a large scatter was observed in the EMR amplitudes even at a minute variation in providing the initial notches. Moreover, fracture test data are known to have large scatter. On the other hand, since the phenomenon of EMR emission has its genesis at atomic level, statistical averaging or adopting standard deviation technique is not advisable for processing of EMR signals. Hence, experiments were repeated six to seven times in each carefully prepared set and the majority of consistent EMR signals were selected for the analysis. Fig.1 shows the specimen configuration under Mode I with antenna position and Fig.2 is a sample printout of one such signal (prior to fracture) with its FFT superimposed.

Effect of rolling direction on EMR emission

The orientation of grains in individual crystal within a metal is ordinarily random. Cold work such as rolling, wire drawing, destroys this randomness of grain orientation. The grain exhibits now a preferred orientation and the material properties are quite different in various directions (anisotropy). The preferred orientations occur under plastic deformation and it is a result of the tendency of slip directions in each grain to align themselves with some common direction of deformation.

Face-centered cubic metals in the cold rolled state are not highly anisotropic, but the tensile strength in the cross section definitely exceeds that in the longitudinal direction for copper and brass, nickel, aluminum, silver, and bronze after severe cold rolling. High tensile and yield strengths and low ductility are usually found in the same directions. Anisotropy increases with the degree of reduction by rolling (Barrett, 1952).

During the present investigations variations of mechanical properties with angle to rolling direction, θ, in 68-32 brass sheets were observed to be almost similar in nature to the properties data presented in (Barrett, 1952). Fig.3 shows the variations of six parameters, viz. $|V_{pmax}|$, V_{RMS}, f, K_I, G_I, and A, all superimposed, with angle to rolling direction θ, for the hard rolled specimens, which show marked changes in behavior at θ~45°. Now the regions near the fractured edges of the specimens, were examined under Scanning Electron Microscope for any microstructural changes, both for θ=0° and 45°. Fig.4 shows the microstructures of these regions of the specimens. It is evident from these figures that hard rolled sheet specimens show α-brass grains along with some deformation twins; however, the β-phase is lesser at θ=45° as compared to θ=0°. It may be noted here that these micrographs are of the regions adjacent to the crack propagation path. Hence Fig.4a, θ=0°, corresponds to the region almost normal to the rolling direction and hence to the direction of applied tension. On the other hand, Fig.4b, θ=45°, corresponds to the region at approximately 45° to the rolling direction, i.e. also at 45° to the applied tension. Therefore, Fig.4a characterizes a brittle zone (fracture) while Fig.4b characterizes a ductile zone. It is well

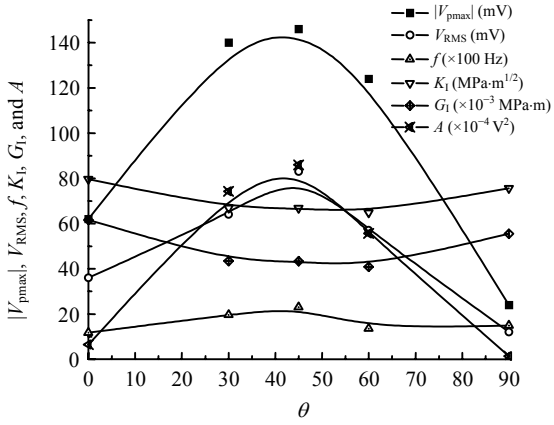

Fig.3 Variations of $|V_{pmax}|$, V_{RMS}, f, K_I, G_I, and A with angle to rolling direction θ, in hard rolled specimens

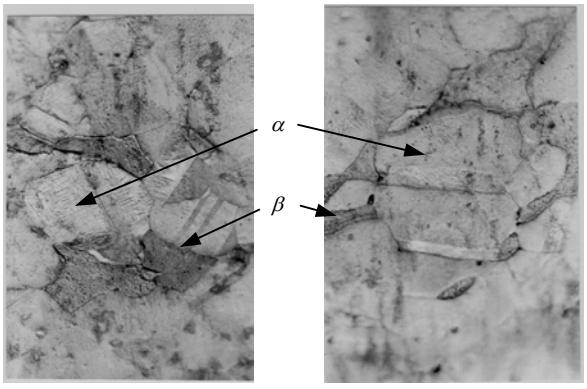

Fig.4 Electron micrographs of the region near fracture edge in specimens. (a) Hard rolled and at θ=0° (magnification ×500); (b) Hard rolled and at θ=45° (magnification ×500)

known that β-phase of Cu-Zn alloy is brittle in nature and α-phase ductile. Therefore, θ=0° specimens should have larger β-phase along the crack propagation region as compared to θ=45°. However, whether the increased β-phase in the crack propagation region of the specimens with θ=0°, has resulted due to any strain-induced phase transformation during plastic deformation and fracture, is not ascertained at this stage of experiments. This requires further investigations. But an inspection of Figs.3 and 4 shows that the EMR responses are enhanced when the crack propagates through α-phase dominated regions.

Effect of zinc addition on EMR emission along different rolling directions

Since the stacking fault energy of an alloy depends on solute content (i.e. changes in the electron to atom ratio), the texture of a metal can change from copper to brass type with increasing alloy additions. Increasing the zinc content in copper can have the effect of a transition in rolling texture from copper to brass type. On the other hand, some researchers argued that the importance of stacking fault energy in controlling the type of deformation texture is related to the relative ease by which cross-slip occurs, the brass texture being generated when cross-slip is more difficult. Others have suggested that the brass texture develops when mechanical twinning or deformation faulting is relatively easy. Therefore, investigations on EMR emissions in this aspect are expected to give some useful information.

Figs.5a~5c show the variations of mechanical parameters, viz. S_{uc}, K_I, and G_I respectively, with the angle to rolling direction θ, for different percentage of zinc addition in copper. The tensile stress at crack unstability, S_{uc}, at every angle of θ, increases with the increase in zinc addition up to 40%, as expected. Variations of K_I and G_I also are in the same pattern. However, there is a marked variation in these parameters when analysed for variations in θ. The graph of 10% zinc addition shows a gradual increase in S_{uc}, K_I, and G_I with a maximum at θ=45°; on the other hand, 20%, 30%, and 40% zinc addition graphs show a gradual decrease in S_{uc}, K_I, and G_I upto θ=45°. It may be noted here that pure copper shows a maximum in both tensile strength and percentage elongation at θ=45° (Barrett, 1952). Hence it is possible that 10% addition of zinc cannot influence the mechanical properties of copper remarkably.

Another point of interest is that in the 20% zinc addition graph. S_{uc}, K_I, and G_I continue to decrease upto θ=45°, and then practically become constant for 45°<θ≤90°; that is, anisotropy in 80-20 Cu-Zn alloy is simple in nature. On the other hand, 70-30 and 60-40 Cu-Zn alloy specimens show a maximum in S_{uc}, K_I, and G_I, with increase in maximum values being much larger in 60-40 Cu-Zn alloy than in 70-30 Cu-Zn alloy.

Figs.5d and 5e are the graphs of the magnitude of EMR amplitude and minimum dominant frequency with the angle to rolling direction θ, at various percent of zinc addition. A careful inspection of the graphs shows the following correlations between EMR responses (amplitude and frequency) and mechanical parameters (S_{uc}, K_I, and G_I):

(1) The EMR amplitude $|V_{pmax}|$, frequency f, S_{uc}, K_I, and G_I, all gradually decrease up to θ≤45° in 60-40, 70-30, and 80-20 Cu-Zn alloys.

(2) All EMR and mechanical parameters then rise and show maximum at θ=60°, and then decrease upto θ=90° in 60-40 and 70-30 Cu-Zn alloys only; the EMR and mechanical parameters remain practically constant for 45°≤θ≤90° in 80-20 Cu-Zn alloy.

(3) On the other hand, $|V_{pmax}|$, frequency f, S_{uc}, K_I, and G_I show a gradual increase of up to θ≤45°, then decline θ=60°, and then remain practically constant upto θ=90°, for 90-10 Cu-Zn alloy.

(4) Therefore, θ=60° to 90°, do not appear to have any influence on these five parameters in 70-30, 80-20, and 90-10 Cu-Zn alloys.

(5) The EMR behaviour of 90-10 Cu-Zn alloy is opposite in nature to those of 80-20, 70-30, and 60-40 Cu-Zn alloys for 0°<θ≤60°.

(6) The EMR frequencies are largest in 70-30 Cu-Zn alloy for all θ, since percent elongation, i.e. ductility is largest in 70-30 Cu-Zn alloy (Smith, 1981), it appears that ductility has a major contribution on EMR frequency.

(7) On the other hand, since tensile strength is largest for 60-40 Cu-Zn alloys, the $|V_{pmax}|$ curve shows that $|V_{pmax}|$ is influenced by both tensile strength and ductility.

(8) The electromagnetic energy release rate is generally proportional to $(|V_{pmax}|)^2$, as has been discussed in the earlier sections. The nature of variations

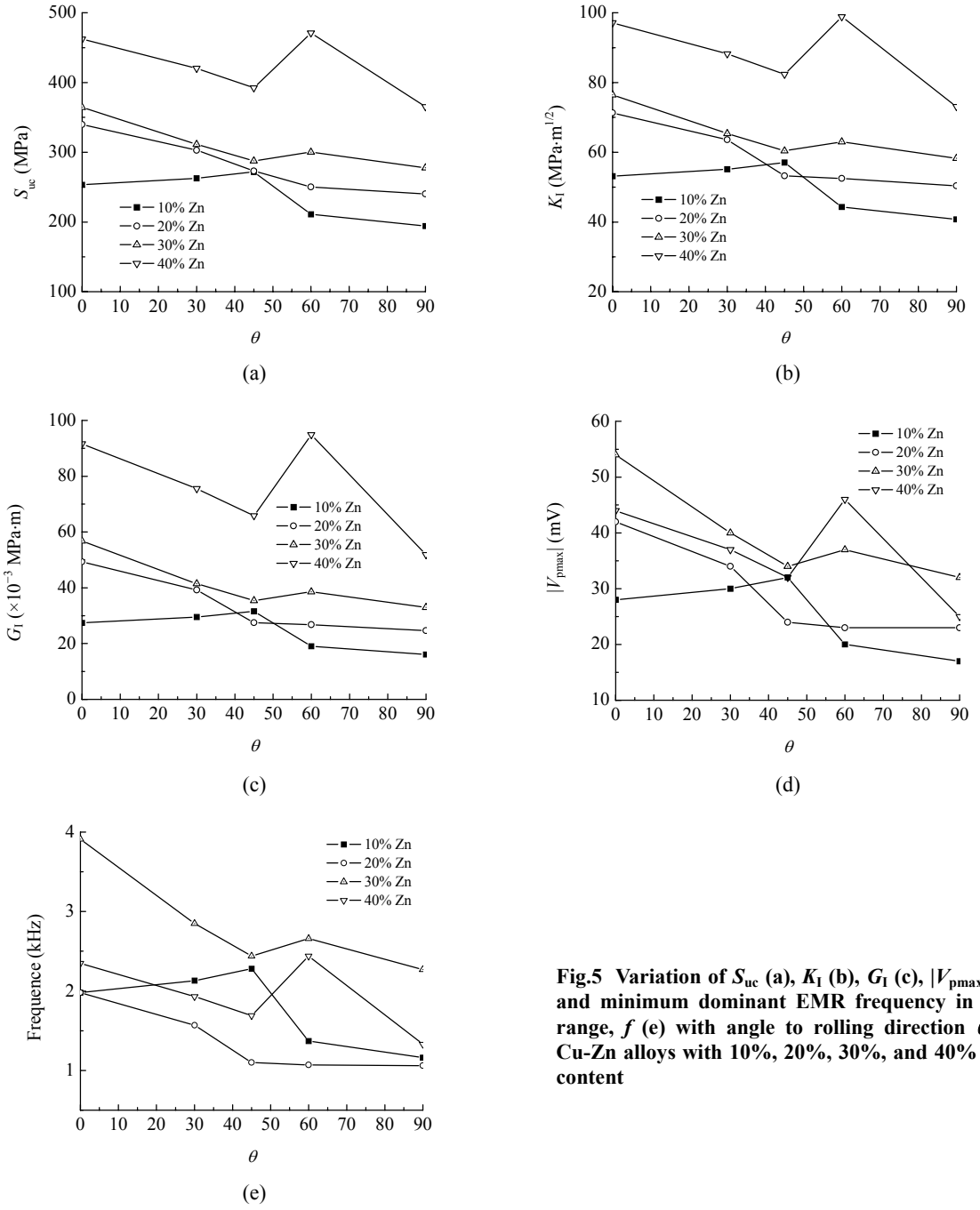

Fig.5 Variation of S_{uc} (a), K_I (b), G_I (c), $|V_{pmax}|$ (d) and minimum dominant EMR frequency in kHz range, f (e) with angle to rolling direction θ, in Cu-Zn alloys with 10%, 20%, 30%, and 40% zinc content

of parameters in Fig.5, therefore, shows that the elastic strain energy release rate can really be correlated to the EMR responses.

(9) Finally it can be safely said that EMR emission phenomenon is anisotropic in nature.

Effect of annealing temperature on EMR emission along different rolling directions

The textures developed in deformed metals by annealing have been studied extensively not only because of their influence on the directionality of properties in the finished products, but also because of their scientific interest.

Barrett (1952) has presented experimental data on the variation of tensile strength, yield strength, elongation and modulus with angle to rolling direction, θ, for the commercial 65-35 brass strips, hard rolled, and annealed for 2 h at 200 °C, 500 °C, and

700 °C respectively. These temperatures are important: the yield strength and tensile strength of 65-35 brass strip annealed 2 h at 200 °C are larger than those of hard-rolled strip; the recrystallization temperature is about 475 °C to 500 °C; and the grain size growth is large at 700 °C. Therefore, for comparison, identically annealed specimens for Mode I test, as described earlier, were investigated.

Variations of mechanical properties with angle to rolling direction, θ, in 68-32 brass sheets of 0.96 mm thickness, hard rolled, and annealed for 2 h at 200 °C, 500 °C, and 700 °C, respectively were almost similar in nature to the graphs presented in (Barrett, 1952). The tensile strength and yield strength of 200 °C annealed specimens were larger than those of hard rolled specimens. The mechanical properties showed anisotropy between θ=30° to θ=60°. Now when K_I and G_I were plotted against θ, Figs.6a and 6b were obtained. It is clear from these figures that the specimens annealed at 500 °C do not show any variation in K_I and G_I with the angle to rolling direction, θ. The hard rolled specimens show marked decrease in K_I and G_I between θ=30° to θ=60°; on the other hand, the 200 °C and 700 °C annealed specimens show a distinct decrease (minima) only at $\theta\cong$45°. It may be noted here that the recrystallization temperature of 68-32 brass is about 475 °C and marked increase in grain size is observed at 700 °C annealing temperature (Callister, 2004).

Figs.6c~6f show the variations of EMR signal parameters, viz. $|V_{pmax}|$, V_{RMS}, A, and f respectively with angle to rolling directions. It is seen that hard rolled specimens show largest anisotropy in all the EMR properties with distinct maxima at θ=45°. The frequency curve, Fig.6f, however shows one minima as well at $\theta\approx$70°. It is further seen that $|V_{pmax}|$, V_{RMS}, and A decrease rapidly with increase in annealing temperature for all θ. This is due to the fact that with increase in annealing temperature the residual stresses resulting from cold rolling decrease substantially and the material becomes softer, behaving more or less isotropically. This results in the reduction in the observed anisotropy. However, the 700 °C annealing temperature specimens show a gradual decrease in all the EMR properties between θ=30° and 60°, and then show practically no change for $\theta\geq$60°. The EMR frequency curve, Fig.6f, is somewhat complex; for example, the 500 °C and 700 °C curves are opposite in nature. Maximum complexity in EMR frequency is observed between θ=45° to 70°. Further experimentations are required to understand the complex behaviour of the EMR frequency.

Figs.3 and 7 show the variations of all the six parameters, temperature-wise, viz. $|V_{pmax}|$, V_{RMS}, f, K_I, G_I, and A, all superimposed, with angle to rolling direction θ, for the specimens hard rolled, and annealed at 500 °C and 700 °C respectively, which show the marked changes in behavior at θ~45°. Now the regions near the fractured edges of the specimens, hard rolled and annealed at 500 °C were examined under Scanning Electron Microscope for any microstructural changes, both for θ=0° and 45°.

Now when the G_I and A data for annealed specimens were normalized on the basis of 200 °C annealed specimen data for θ=0°, Fig.8 is obtained. This once again shows a close similarity between the elastic strain energy release rate G_I and the EMR energy release rate A. However, data for hard-rolled sheets did not fit into the curve of Fig.8 drawn for annealed specimens. Therefore, fresh specimens annealed at 400 °C temperature were further investigated and included in Fig.8 for cross-checking of the results which fitted well into the curve. A large deviation was observed for other values of θ. Thus, the entire experimental results showed that the evaluation of elastic strain energy release rate G_I can be made through the measurement of the EMR energy release rate, A, provided specimens are prepared with their longitudinal axis along the rolling direction (θ=0°) and with similar processing history.

CONCLUSION

On the basis of the results presented in the earlier sections, the following conclusions were drawn:

(1) Distinct EMR signals were emitted from Cu-Zn alloy specimens during Mode I fracture and the parameters for investigations were evaluated on the basis of the last signal, obtained prior to fracture;

(2) A total of seven parameters were analysed: maximum stress at the crack tip instability, S_{uc}; stress intensity factor, K_I; elastic strain energy release rate, G_I; EMR peak amplitude, $|V_{pmax}|$, RMS value of EMR voltage, V_{RMS}; EMR frequency, f; and electromagnetic energy release rate, A;

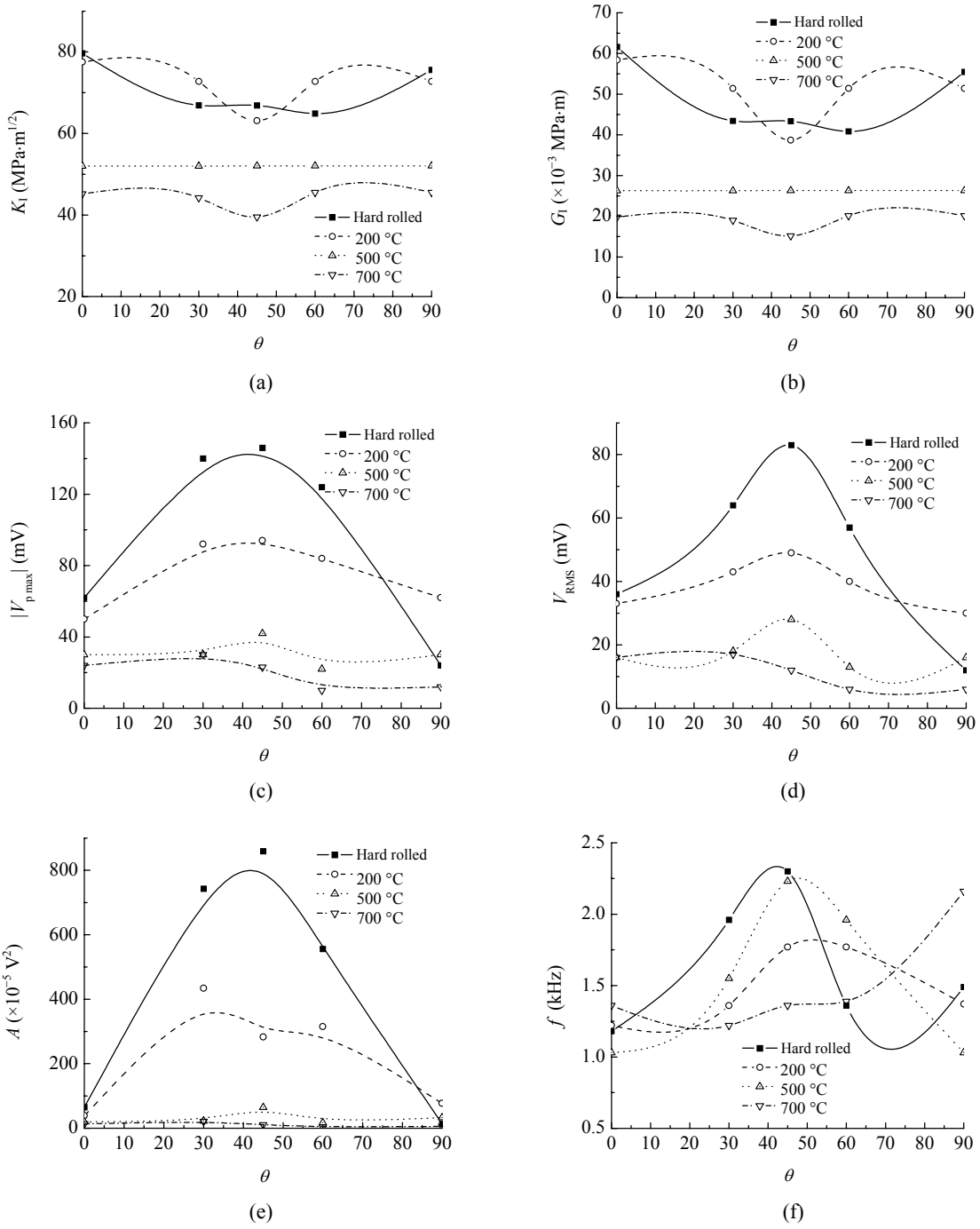

Fig.6 Variation of K_I (a), G_I (b), $|V_{pmax}|$ (c), V_{RMS} (d), average EMR energy release rate A (e) and minimum dominant EMR frequency in kHz range, f (f) with angle to rolling direction θ, in specimens, hard rolled, and annealed at 200 °C, 500 °C, and 700 °C respectively

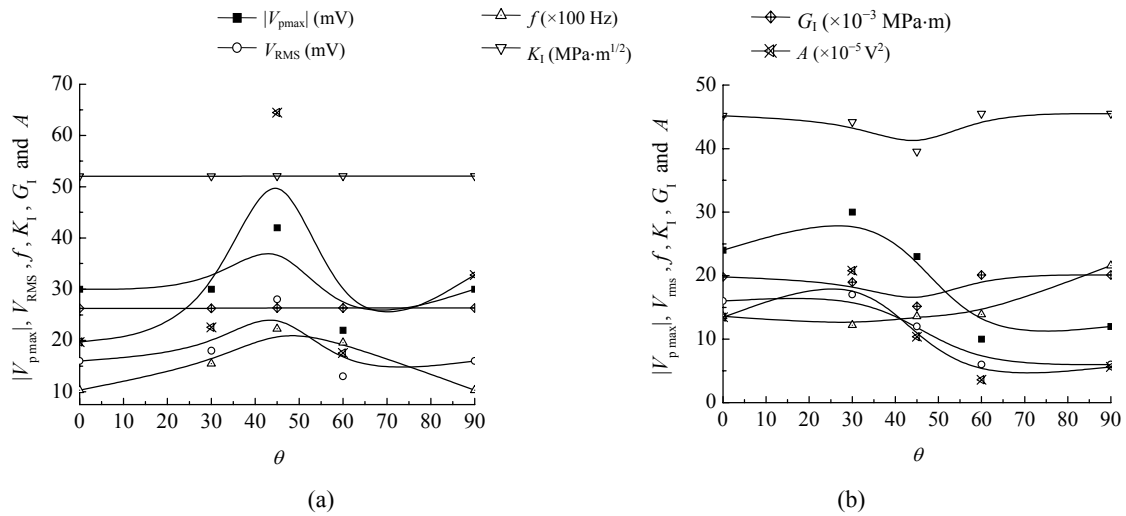

Fig.7 Variations of $|V_{pmax}|$, V_{RMS}, f, K_I, G_I, and A with angle to rolling direction θ, in specimens annealed at 500 °C (a) and 700 °C (b)

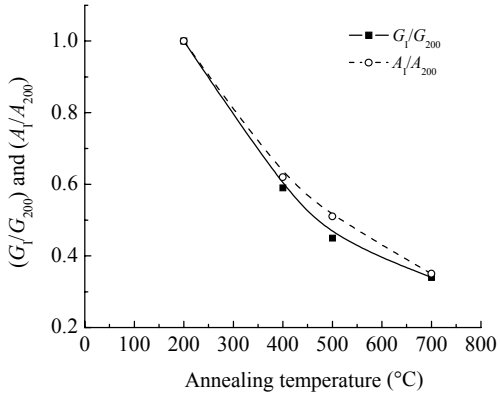

Fig.8 Variations of the normalized values of G_I and A_I with annealing temperature for specimens with θ=0°

(3) EMR emission was observed to be anisotropic in nature; all parameters, $|V_{pmax}|$, V_{RMS}, f, K_I, G_I, and A showed marked changes in the behaviour at angle to rolling direction, θ~45°; microstructural changes, such as deformation twins, were observed in the fracture zone of the specimens at θ~45°;

(4) Significant changes in both mechanical and EMR parameters were observed in Cu-Zn alloys with increasing zinc content; all parameters gradually decreased upto $\theta \leq 45°$, and then showed maxima at around θ=60°, and practically remained constant for $60° \leq \theta \leq 90°$; on the other hand, 90-10 Cu-Zn alloy specimens showed the opposite trend;

(5) $|V_{pmax}|$, V_{RMS}, and A showed rapid decrease with increase in annealing temperature; however, specimens annealed at 700 °C showed a gradual decrease in all the EMR properties between θ=30° and 60°, and then practically showed no changes for higher values of θ;

(6) All specimens with various annealing temperatures also exhibited marked changes at θ~45°; specimens annealed at 500 °C, θ=0°, showed some bigger β-grains than hard rolled specimens, with deformation twins completely absent;

(7) G_I and A were observed to be very closely interrelated. Therefore, an evaluation of A may lead to a novel technique for the determination of fracture toughness for hard-rolled sheets.

References

Barrett, C.S., 1952. Structure of Metals. Mc-Graw Hill Book Company, New York, p.521-523.

Callister, W.D.Jr., 2004. Materials Science and Engineering: An Introduction. John Wiley & Sons (Asia) Pte. Ltd., Singapore, p.183-184.

Haykin, S., van Veen, B., 2002. Signals and Systems. John Wiley, Singapore.

Hertzberg, R.W., 1996. Deformation and Fracture Mechanics of Engineering Materials. John Wiley & Sons, New York, p.321-336.

Jagasivamani, V., 1987. Some Studies on Electromagnetic and Acoustic Emission Associated with Deformation and Fracture of Metallic Materials. Ph.D Thesis, Indian Institute of Technology, Chennai, India.

Jagasivamani, V., Iyer, K.J., 1988. Electromagnetic emission during the fracture of heat treated spring steel. *Materials Letters*, **6**(11-12):418-422. [doi:10.1016/0167-577X(88)90043-2]

Kumar, R., Misra, A., 2006. A New Approach for Smart Sensors in Design against Metallic Failure. Proceedings

of the International Conference on Resource Utilisation and Intelligent Systems, Erode, India, p.565-569.

Mishra, D., Misra, A., 1980. Stress-induced electromagnetic effect—A new biophysical application to head injury. *Neurology India*, **XXVIII**:234-241.

Misra, A., 1973. On the magnetism produced in unmagnetized iron specimens at breakage under tension. *Indian Journal of Pure and Applied Physics*, **11**:419-422.

Misra, A., 1975a. Electromagnetic effects at metallic fracture. *Nature*, **254**(5496):133-134. [doi:10.1038/254133a0]

Misra, A., 1975b. Ninth Yearbook to the Encyclopedia of Science and Technology. Edizioni Scientifiche E Tecniche, Mondadori, Italy.

Misra, A., 1976. Discovery of Stress-induced Magnetic and Electromagnetic Effects in Metals. D.Sc. Thesis, Ranchi University.

Misra, A., 1977. Theoretical study of the fracture-induced magnetic effect in ferromagnetic materials. *Physics Letters*, **62A**:234-236.

Misra, A., 1978. A physical model for the stress-induced electromagnetic effect in metals. *Applied Physics*, **16**:195-199. [doi:10.1007/BF00930387]

Misra, A., 1981. Stress-induced magnetic and electromagnetic effects in metals. *Journal of Scientific and Industrial Research*, **40**:22-23.

Misra, A., Ghosh, S., 1980a. Electron plasma model for the electromagnetic effect at metallic fracture. *Indian Journal of Pure and Applied Physics*, **18**:851-856.

Misra, A., Ghosh, S., 1980b. electromagnetic radiation characteristics during fatigue crack propagation and fracture. *Applied Physics*, **23**(4):387-390. [doi:10.1007/BF00903221]

Misra, A., Varshney, B.G., 1990. Can a stress alone applied to a demagnetized ferromagnetic specimen produce any magnetization. *Journal of Magnetism and Magnetic Materials*, **89**(1-2):159-165. [doi:10.1016/0304-8853(90)90720-B]

Misra, A., Kumar, A., 2004. Some basic aspects of electromagnetic radiation during crack propagation in metals. *International Journal of Fracture*, **127**(4):387-401. [doi:10.1023/B:FRAC.0000037676.32062.cb]

Molotskii, M.I., 1980. Dislocation mechanism for the Misra effect. *Soviet Technical Physics Letters*, **6**:22-23.

Smith, W.F., 1981. Structure and Properties of Engineering Alloys. Mc-Graw Hill, New York.

Srilakshmi, B., Misra, A., 2005a. Secondary electromagnetic radiation during plastic deformation and crack propagation in uncoated and tin-coated plain-carbon steel. *Journal of Materials Science*, **40**(23):6079-6086. [doi:10.1007/s10853-005-1293-4]

Srilakshmi, B., Misra, A., 2005b. Electromagnetic radiation during opening and shearing modes of fracture in commercially pure aluminum at elevated temperature. *Materials Science and Engineering A*, **404**(1-2):99-107. [doi:10.1016/j.msea.2005.05.100]

Srilakshmi, B., Misra, A., 2005c. Effects of some fracture mechanics parameters on the emission of electromagnetic radiation from commercially pure aluminum. *Manufacturing Technology and Research—An International Journal*, **1**:97-104.

Srilakshmi, B., Misra, A., 2005d. Electromagnetic Radiation during Crack Propagation in Metals—A New Trend in the Development of Smart Materials. Proceedings of International Symposium on Smart Materials and Systems, Chennai, India, p.219-229.

Tudik, A.A., Valuev, N.P., 1980. Electromagnetic emission during the fracture of metals. *Soviet Technical Physics Letters*, **6**:37-38.